Bioelectrochemistry 80 (2011) 114–120

Contents lists available at ScienceDirect

Bioelectrochemistry

journal homepage: www.elsevier.com/locate/bioelechem

Amperometric glucose sensor based on glucose oxidase immobilized on gelatin-multiwalled carbon nanotube modified glassy carbon electrode

Arun Prakash Periasamy, Yu-Jung Chang, Shen-Ming Chen *

Department of Chemical Engineering and Biotechnology, National Taipei University of Technology, No.1, Section 3, Chung-Hsiao East Road, Taipei 106, Taiwan, ROC

ARTICLE INFO

Article history:
Received 22 April 2010
Received in revised form 16 June 2010
Accepted 18 June 2010
Available online 26 June 2010

Keywords:
Direct electrochemistry
Glucose oxidase
Gelatin
Multiwalled carbon nanotubes
Electrocatalysis

ABSTRACT

We investigated the direct electrochemistry of glucose oxidase (GOx) at gelatin-multiwalled carbon nanotube (GCNT) modified glassy carbon electrode (GCE). GOx was covalently immobilized onto GCNT modified GCE through the well known glutaraldehyde (GAD) chemistry. The immobilized GOx showed a pair of well-defined reversible redox peaks with a formal potential ($E^{0\prime}$) of −0.40 V and a peak to peak separation (ΔE_p) of 47 mV. The surface coverage concentration (Γ) of GOx in GCNT/GOx/GAD composite film modified GCE was 3.88×10^{-9} mol cm^{-2} which indicates the high enzyme loading. The electron transfer rate constant (k_s) of GOx immobilized onto GCNT was 1.08 s^{-1} which validates a rapid electron transfer processes. The composite film shows linear response towards 6.30 to 20.09 mM glucose. We observed a good sensitivity of 2.47 μA mM^{-1} cm^{-2} for glucose at the composite film. The fabricated biosensor displayed two weeks stability. Moreover, it shows no response to 0.5 mM of ascorbic acid (AA), uric acid (UA), acetaminophen (AP), pyruvate (PA) and lactate (LA) which shows its potential application in the determination of glucose from human serum samples. The composite film exhibits excellent recovery for glucose in human serum at physiological pH with good practical applicability.

1. Introduction

In recent years, rapid and accurate monitoring of blood glucose level is required for the control of diabetes. Among various electronic devices commercially available in the market, with low-cost of production, rapid response, high sensitivity and good selectivity, glucose oxidase (GOx) based enzyme sensors have been widely employed to monitor the blood glucose level [1]. However, one of the most challenging aspects in the development of highly sensitive glucose sensor is the selection of a suitable matrix for GOx immobilization. With high mechanical strength, excellent conductivity and antifouling properties, multiwalled carbon nanotubes (MWCNTs) have been immensely used in glucose sensors for GOx immobilization [2]. Some of the recently reported MWCNT matrices for GOx immobilization are ionic liquid n-octylpyridinum hexafluorophosphate dispersed MWCNT [3], MWCNT/gold nanoparticles-Teflon composites [4], Chitosan dispersed MWCNT [5], gold nanoparticles/thiol group functionalized MWCNT/Chitosan-ionic liquid [6], cobalt hexacyanoferrate nanoparticles/gold nanoparticles (seed)/MWCNT composites [7], crystalline gold nanoparticles modified MWCNT [8], platinum nanoparticle/MWCNT composites [9], nitrogen doped MWCNT [10] and polymerized ionic liquid-wrapped MWCNT [11]. The inclusion of MWCNT into the immobilization matrix leads to the high sensitivity and good stability of the immobilized enzyme [3]. In addition, MWCNT platform offers more compatible environment to the immobilized GOx and thereby favors the rapid shuttling of electrons with the electrode surface [12]. Though the MWCNT based glucose sensors possess high sensitivity and good electrocatalytic activity they have a major drawback that the prepared MWCNT dispersions precipitate on long storage and are not quite stable. Further, the dispersing agents may cause the electrode surface passive or cause any damage to the walls of MWCNT. Thus there is a need for exploring a suitable dispersing agent for MWCNT.

Gelatin is the chief protein present in skin, bones and white connective tissues which is generally separated by the partial hydrolysis of collagen [13]. It is extremely heterogeneous; composed of polypeptides of various sizes and it possesses a molecular weight distribution in the range of 15,000 to 250,000. Previously, Zheng and Zheng reported that the immobilization of non-polar amino acid chain of gelatin at the side wall of MWCNT takes place through hydrophobic–hydrophobic interactions and which leads to the formation of stable dispersion of MWCNT [14]. In addition, other related reports found elsewhere in the literature substantiate that the stability of the MWCNT/gelatin dispersion could be comprehensively augmented by increasing the amount of MWCNT [15,16]. Considering such advantageous properties, in the present study, we prepared a stable MWCNT dispersion using gelatin as the dispersing agent. For the first time, we utilized the gelatin dispersed MWCNT (GCNT) matrix to immobilize the model enzyme GOx. We noticed a rapid direct electron transfer processes between GOx and the glassy carbon electrode (GCE). Further, a good linear range and

* Corresponding author. Tel.: +886 2270 17147; fax: +886 2270 25238.
E-mail address: smchen78@ms15.hinet.net (S.-M. Chen).

1567-5394/$ – see front matter © 2010 Elsevier B.V. All rights reserved.
doi:10.1016/j.bioelechem.2010.06.009

reasonable sensitivity for glucose was observed at the composite film with GCNT. The good performance of this glucose sensor could be attributed to the stability of GCNT and this opens up new horizons in the field of functionalized MWCNT based glucose sensor related researches.

2. Experimental

2.1. Reagents and apparatus

GOx, type X-S from *Aspergillus niger* and gelatin from porcine skin, type A were purchased from Sigma-Aldrich and used as received. MWCNT with O.D. 10–15 nm, I.D. 2–6 nm, and length 0.1–10 μm was obtained from Aldrich and used without further purification. 25 wt.% glutaraldehyde (GAD) solution in water was obtained from Sigma-Aldrich. D(+) glucose (*Dextrose, anhydrous*) and acetaminophen were purchased from Wako pure chemical Industries, Ltd. Ascorbic acid, uric acid and L (+) lactic acid (98%) were obtained from Sigma-Aldrich. Sodium pyruvate solution, 100 mM, sterile-filtered, cell culture tested was also obtained from Sigma-Aldrich. The supporting electrolyte used for all experiments is pH 7 phosphate buffer solution (PBS) prepared using 0.05 M Na_2HPO_4 and NaH_2PO_4 solutions. All the reagents used were of analytical grade and doubly distilled water was utilized for the preparation of all aqueous solutions.

Electrochemical studies were performed in a conventional three electrode cell. Prior to each experiment, all solutions were deoxygenated by passing pre-purified N_2 gas for 10 min. Cyclic voltammetry (CV) studies were carried out using CHI 1205a work station. BAS GCE with an electrode surface area of 0.079 cm^2 was used as working electrode and Pt wire with 0.5 mm diameter was used as counter electrode. All the potentials were referred with respect to standard Ag/AgCl reference electrode. IM6ex ZAHNER (Kroanch, Germany) was used for electrochemical impedance spectroscopy (EIS) studies. CHI-750 potentiostat was used for amperometric i–t curve studies. Surface morphology of the prepared GCNT was studied using JEM 2007 model transmission electron microscope (TEM). Hitachi S-3000 H scanning electron microscope (SEM) and Being nano-instruments CSPM 4000, atomic force microscope (AFM) were employed for the surface morphological characterization of GOx, GCNT/GOx/GAD and DCNT/GOx/GAD films.

2.2. Fabrication of GCNT/GOx/GAD composite film

GCNT used in this work was prepared according to the procedure reported elsewhere in the literature [14]. Briefly, 10 mg of MWCNT was dispersed into 1 mg mL^{-1} of aqueous gelatin solution and the resulting mixture was ultrasonicated for 1 h, until a homogeneous, black dispersion containing 2 mg mL^{-1} MWCNT was obtained. 0.25% GAD and 10 mg mL^{-1} GOx solutions were prepared in PBS and stored at 4 °C. Prior to electrode modification, GCE surface was polished well on a clean Buehler polishing cloth using 0.05 μm alumina slurry. The polished GCE surface was washed several times with double distilled water, ultrasonicated for 10 min and finally dried at room temperature. The cleaned GCE was then used for the fabrication of GCNT/GOx/GAD composite film. About 0.13 mL cm^{-2} of GCNT was drop casted above the pre-cleaned GCE surface and dried. Then 0.05 mL cm^{-2} of GOx solution was spread gently over the GCNT modified GCE and the enzyme solution was left to dry for 10 min at 35 °C. Finally, 0.03 mL cm^{-2} of 0.25% GAD solution was drop casted above the GOx modified GCE and dried for 10 min. The free $-NH_2$ group of GOx and –CHO group of GAD react to form the covalent linkage at the GCNT matrix (see Fig S1 supplementary data). Thus GOx has been covalently immobilized at the GCNT matrix through GAD cross-linking. The obtained GCNT/GOx/GAD composite film modified GCE was then gently rinsed a few times with double distilled water and used for further experiments. In order to investigate the importance of using GCNT as immobilization matrix, MWCNT without gelatin coating has also been prepared. For this purpose, about 10 mg of MWCNT was dispersed into 10 mL of *N,N*-dimethylformamide (DMF) solution and then ultrasonicated for 1 h. The DMF dispersed MWCNT (DCNT) was then used for the fabrication of DCNT/GOx/GAD film on GCE following the similar fabrication procedure employed for GCNT/GOx/GAD composite film.

3. Results and discussions

3.1. Direct electrochemistry of GOx

Fig. 1 shows the cyclic voltammograms obtained at bare, GCNT, DCNT, DCNT/GOx/GAD and GCNT/GOx/GAD film modified GCEs in deoxygenated PBS at the scan rate of 50 mV s^{-1}. Cyclic voltammograms were recorded in the potential range of −0.8 to 0.2 V. Initially, the GCNT loading was optimized through CV studies for the efficient immobilization of GOx. The effect of GCNT loading on cathodic peak current (I_{pc}) at GCNT/GOx/GAD composite film modified GCE is shown in Fig. 1 inset. It is obvious from the inset plot that Ipc increases with increase in the amount of GCNT. Maximum I_{pc} is observed for 20 μg cm^{-2} of GCNT i.e. 0.13 mL cm^{-2} of GCNT. This optimized amount of GCNT is used for all experiments. In Fig. 1, in the absence of GOx, no significant redox peaks are noticed in this potential range for bare, GCNT or DCNT modified GCEs. The GOx/GAD film too exhibits no redox peaks. Interestingly, a pair of well-defined redox peaks with maximum peak current is observed at GCNT/GOx/GAD composite film modified GCE in the same potential window. $E^{0\prime}$ associated with this redox couple is −0.40 V which is close to the $E^{0\prime}$ of other GOx modified electrodes reported previously [17–19]. The peak to peak separation (ΔE_p) is 47 mV. This redox couple could be thus attributed to the direct electron transfer of GOx at the GCNT modified GCE surface. A similar redox couple with much lowered peak current is observed at DCNT/GOx/GAD film on GCE. $E^{0\prime}$ for this redox couple is −0.41 V and ΔE_p is 33 mV. The higher redox peak current observed at GCNT/GOx/GAD composite film on GCE shows a faster electron transfer process. Furthermore, the surface coverage concentration (Γ)

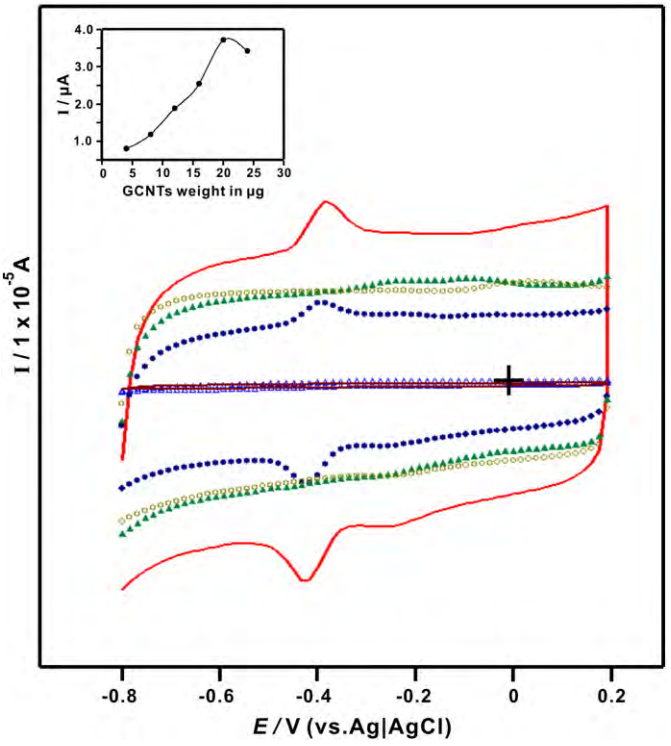

Fig. 1. Cyclic voltammograms obtained at bare GCE (▬), GOx/GAD (△), DCNT/GOx/GAD (■), GCNT (○), DCNT (▲) and GCNT/GOx/GAD (▬) film modified GCEs in deoxygenated PBS at 50 mV s^{-1} scan rate. Inset shows the influence of GCNT loading on I_{pc} observed at GCNT/GOx/GAD composite film modified GCE.

of GOx at both GCNT/GOx/GAD and DCNT/GOx/GAD modified GCEs has been calculated. The maximum Γ value of 3.88×10^{-9} mol cm^{-2} is observed at GCNT/GOx/GAD composite film on GCE which is 33.12% higher than that of DCNT/GOx/GAD film ($\Gamma=2.59\times10^{-9}$ mol cm^{-2}). This shows higher enzyme loading at the GCNT/GOx/GAD composite film.

3.2. Different scan rate studies

Fig. 2 shows the cyclic voltammograms of GCNT/GOx/GAD composite film modified GCE in deoxygenated PBS at different scan rates. Both I_{pa} and I_{pc} increase linearly with increase in scan rates from 20 to 200 mV s^{-1}. This indicates that the electron transfer process occurring at GCNT/GOx/GAD composite film on GCE is a surface confined process. Fig. 2 inset shows the linear dependence of I_{pa} and I_{pc} on different scan rates from 20 to 200 mV s^{-1}. The electron transfer rate constant (k_s) for GOx at GCNT/GOx/GAD composite film modified GCE is calculated using Laviron equation [20].

$$\mathrm{Log}\, k_s = \alpha\,\mathrm{Log}\,(1-\alpha) + (1-\alpha)\mathrm{Log}\,\alpha - \mathrm{Log}\,(RT/nF\nu) - \alpha\,(1-\alpha)\,nF\Delta E_p/2.3\,RT. \quad (1)$$

Where, R is the gas constant (8.314 J mol^{-1} K^{-1}), T is the room temperature (298.15 K) and ΔE_p is the peak separation of the FAD/$FADH_2$ redox couple. Here, α value is assumed as ≈0.5 and the number of electrons transferred is considered as 2. The k_s value at GCNT/GOx/GAD composite film on GCE is calculated to be 1.08 s^{-1} and it is higher than that reported by Yao and Shiu for GOx immobilized at MWCNT-gold colloid composites with poly (diallydimethylammonium chloride) (PDDA) coatings ($k_s=1.01$ s^{-1}) [19]. This result shows that GCNT matrices efficiently facilitate electron transfer process between GOx and the electrode surface.

3.3. Effect of pH

Fig. 3 shows the effect of pH on GOx (FAD/$FADH_2$) redox couple at GCNT/GOx/GAD composite film modified GCE in various buffer solutions (pH 1 to 11). The redox peak current remains stable in the pH range of 1 to 11. The redox couple is also reproducible when the composite film modified GCE is transferred from one buffer solution to another. The influence of pH over the anodic peak potential (E_{pa}), cathodic peak potential (E_{pc}) and $E^{0\prime}$ of FAD/$FADH_2$ redox couple at GCNT/GOx/GAD composite film modified GCE is shown in Fig. 3 inset. From the inset plot of $E^{0\prime}$ vs. pH, it is apparent that both E_{pa}, E_{pc} and $E^{0\prime}$ exhibit a linear dependence over different pHs. The correlation coefficient is 0.987. The slope value is found to be −49 mV/pH which is closer to −50.3 and −50.9 mV/pH reported for GOx immobilized at bamboo shaped MWCNT and poly(diallydimethylammonium) chloride (PDDA) wrapped MWCNT respectively [21,22]. It is also close to the theoretical value of Nernstian equation for equal number of proton and electron transfer process. Thus the FAD/$FADH_2$ redox couple reported in this study is an equal number of proton and electron transfer processes.

3.4. Surface morphological characterizations using TEM, SEM and AFM studies

TEM study has been carried out to investigate the surface morphology of the prepared GCNTs. Fig. S2 shows the TEM image of GCNT at 10 nm magnification. It is clear from Fig. S2 that GCNTs are well dispersed in aqueous gelatin solution and they retain their well-defined nanostructures. The outer wall of MWCNT is coated well with gelatin. The gelatin coating around the walls of MWCNT offers good biocompatibility to the immobilized GOx. As reported previously by Zheng and Zheng the good stability of MWCNTs in aqueous gelatin solution could be attributed to the strong interactions between the hydrophobic amino acid chain of gelatin and hydrophobic side walls of MWCNTs.

Prior to AFM and SEM analyses, ITO surfaces were cleaned well, sonicated in acetone–water mixture for 15 min and then dried. GOx, DCNT/GOx/GAD and GCNT/GOx/GAD films were fabricated on clean ITO surface. Then dried at 25 °C and used for AFM and SEM characterizations. Fig. 4(a) and (a′) shows the AFM and SEM images of only GOx film. Small spherical voids surrounded by small bead like structures are seen on the film surface. Whereas the AFM and SEM images of DCNT/GOx/GAD film coated ITO show large bead like structures without any spherical voids (See Fig. 4 (b) and (b′)). This may be due to the filling up of the voids by the GAD. Similarly, Fig. 4(c)

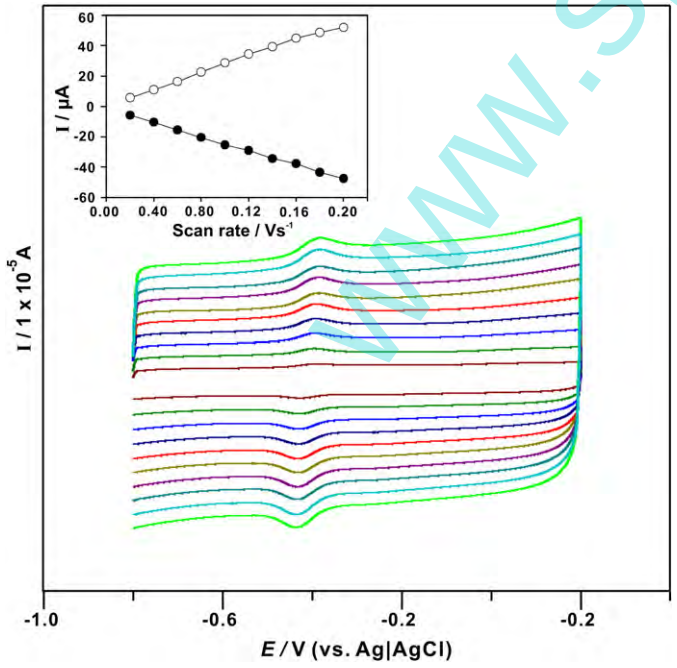

Fig. 2. Cyclic voltammograms recorded at GCNT/GOx/GAD composite film modified GCE in deoxygenated PBS at different scan rates. The scan rates from inner to outer are: 20, 40, 60, 80, 100, 120, 140, 160, 180 and 200 mV s^{-1}. Inset shows the linear dependence of I_{pa} (●) and I_{pc} (○) on scan rate (20 to 200 mV s^{-1}).

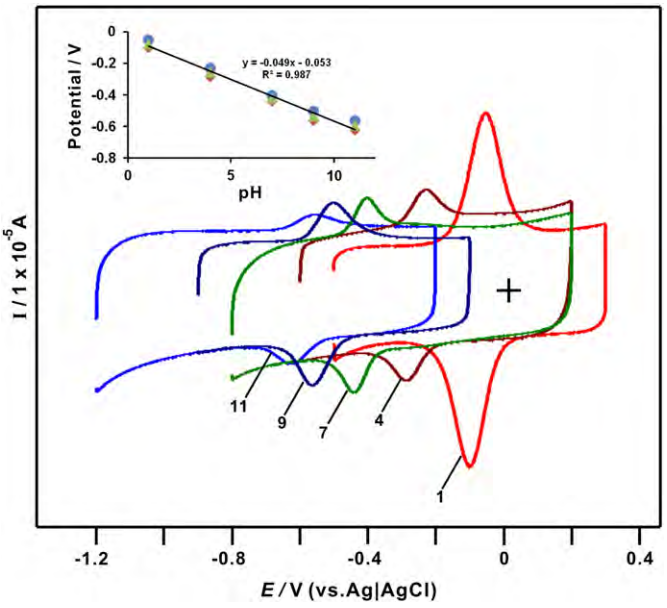

Fig. 3. Cyclic voltammograms obtained at GCNT/GOx/GAD composite film modified GCE in deoxygenated various buffer solutions (pH 1–11) at the scan rate of 50 mV s^{-1}. Inset shows the influence of pH on E_{pa} (●), E_{pc} (■) and $E^{0\prime}$ (▲) of GCNT/GOx/GAD composite film.

and (c′) shows the AFM and SEM images of uniform GCNT/GOx/GAD composite film coated ITO. Here, closely packed larger bead like structures are seen. This validates higher GOx loading at GCNT matrix and it could be attributed to the larger surface area of GCNT. Thus SEM and AFM studies reveal the discriminate surface morphology between GOx, DCNT/GOx/GAD and DCNT/GOx/GAD films.

3.5. EIS studies at different film modified GCEs

The GOx immobilization and its loading at various modified electrode surfaces have been investigated using EIS. Fig. 5(a) shows the real and imaginary part of the impedance spectra represented as Nyquist plots (Z_{im} vs. Z_{re}) for only GOx, DCNT/GOx/GAD and GCNT/GOx/GAD film modified GCEs in PBS containing 5 mM $Fe(CN)_6^{3-/4-}$. The inset shows the Randles equivalence circuit model. In the Nyquist plot, a semicircle portion results from the parallel combination of electron transfer resistance (R_{et}) and double layer capacitance (C_{dl}) resulting from electrode impedance [23]. In the present study, EIS of GOx modified GCE exhibits a larger semicircle as shown in Fig. 5(a). Whereas, depressed semicircle with smaller diameter is observed at bare/GCE (see Fig. 5(b)). This indicates that greater hindrance to electron transfer occurs at the GOx modified GCE rather than bare/GCE. The increased electron transfer resistance observed at GOx modified GCE could be due to the thick protein layer surrounding the FAD redox centre of GOx [24]. Interestingly, no significant semicircles are noticed at both DCNT/GOx/GAD and GCNT/GOx/GAD film

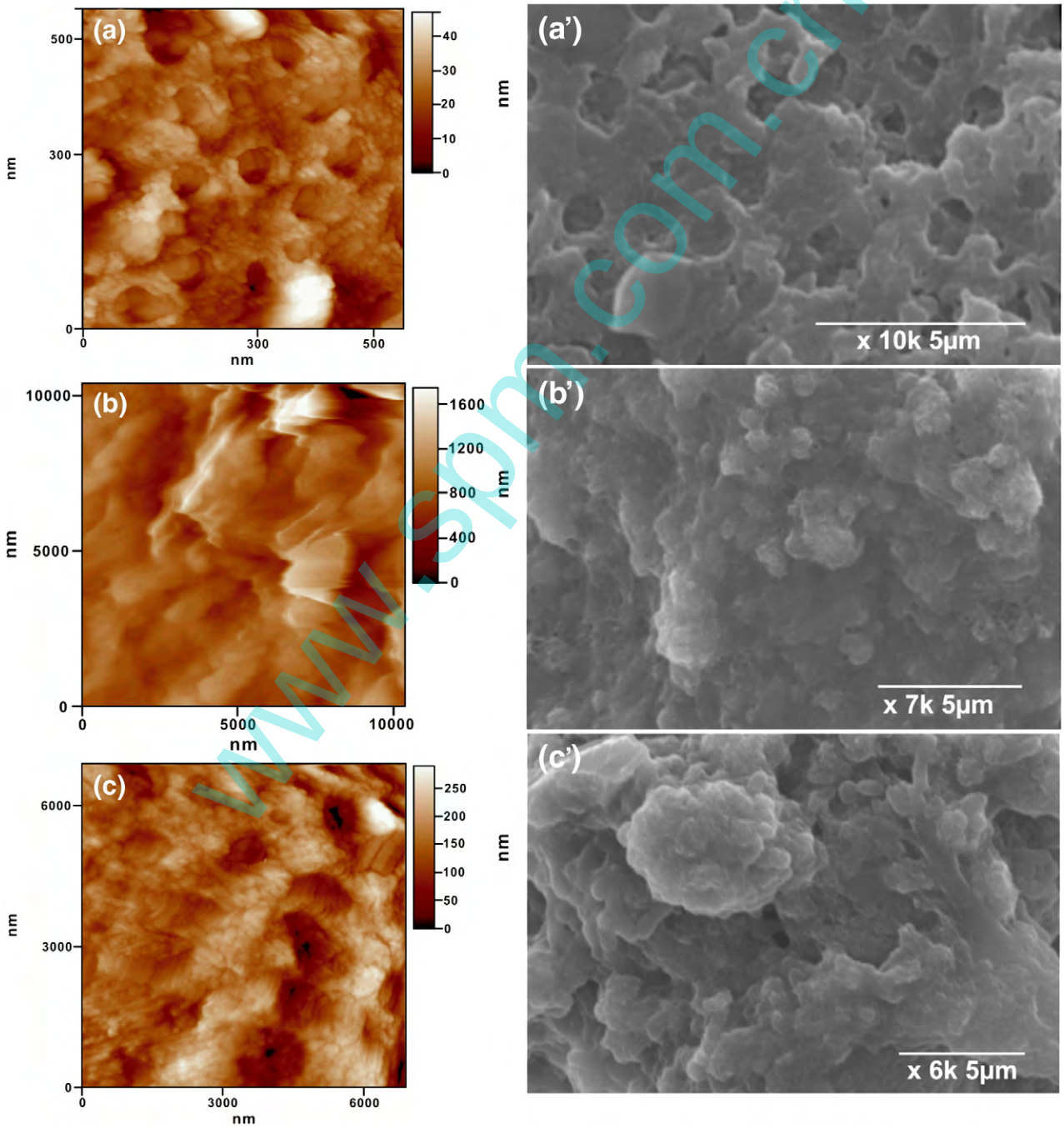

Fig. 4. AFM images of (a) GOx, (b) DCNT/GOx/GAD and (c) GCNT/GOx/GAD films. SEM images of (a′) GOx, (b′) DCNT/GOx/GAD and (c′) GCNT/GOx/GAD films.

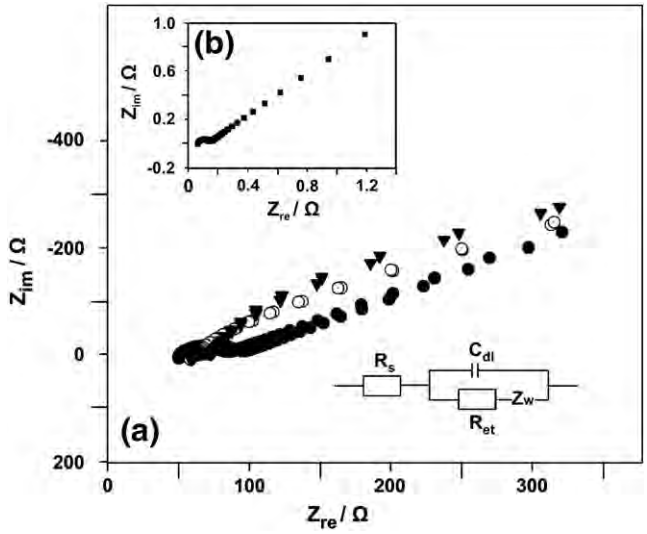

Fig. 5. (a) EIS of GOx (●), DCNT/GOx/GAD (○) and GCNT/GOx/GAD (▼) film modified GCEs in PBS containing 5 mM $Fe(CN)_6^{3-}/Fe(CN)_6^{4-}$. (b) Shows the EIS of bare/GCE (■) in PBS containing 5 mM $Fe(CN)_6^{3-}/Fe(CN)_6^{4-}$. Frequency: 0.1 Hz to 100 kHz. Inset shows the Randles circuit for above modified GCEs.

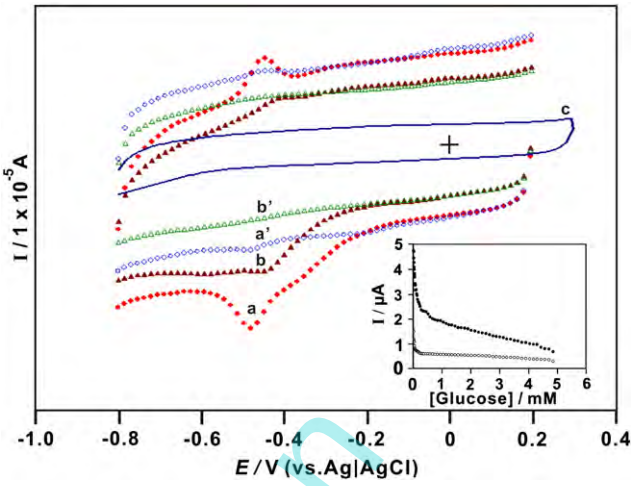

Fig. 6. Cyclic voltammograms recorded at GCNT/GOx/GAD composite film modified GCE in (a) 0.05 and (b) 4.3 μM glucose containing oxygenated PBS. Scan rate: 50 mV s^{-1}. Similarly, cyclic voltammograms obtained at DCNT/GOx/GAD film modified GCE in (a′) 0.05 and (b′) 4.3 μM glucose containing PBS under similar conditions as in (a) and (b). (c) Represents the electrocatalytic response of bare/GCE in highest glucose concentration (4.3 μM). Inset plot shows the linear dependence of peak current vs. [glucose]/μM for GCNT/GOx/GAD (●) and DCNT/GOx/GAD (○) film modified GCEs.

modified GCEs in this frequency range (see Fig. 5(a)). This shows that rapid electron transfer occurs at these modified GCEs which are attributed to the excellent conductivity of GCNT and DCNT.

The R_{et} and C_{dl} values calculated for various modified GCEs are presented in Table S1. From Table S1 it is obvious that, lowest R_{et} value is observed at GCNT modified GCE i.e., $R_{et} = 2.77\ \Omega$. Comparatively, DCNT modified GCE possesses about 17 times higher R_{et} value i.e. 48.88 Ω. The lower R_{et} value observed at GCNT modified GCE validates the higher conductance of GCNT than DCNT. In contrast, the R_{et} value noticed at GCNT/GOx/GAD modified GCE is found to be higher than that of DCNT/GOx/GAD and any other modified GCEs discussed in Table S1 (except GOx/GCE). The higher R_{et} value observed at GCNT/GOx/GAD composite film modified GCE could be due to the more amount of GOx present on the electrode surface which hinders the electron transfer. Thus EIS studies show that more amount of GOx is well immobilized at the GCNT/GOx/GAD composite film, which is in good agreement with the surface coverage studies discussed in Section 3.1.

3.6. Electrocatalysis of GCNT/GOx/GAD composite film towards oxygen reduction and glucose determination

The influence of dissolved oxygen at GCNT/GOx/GAD composite film modified GCE in deoxygenated and oxygenated PBS is shown in Fig. S3 (a) and (b) (see supplementary data). From the results it is obvious that the reduction peak current observed at GCNT/GOx/GAD composite film modified GCE in oxygenated PBS is higher than that observed in deoxygenated PBS. This result reveals that dissolved oxygen is reduced effectively at GCNT/GOx/GAD composite film. Similar observations have been reported at GOx modified electrodes [17,25]. Further, the electrocatalytic response towards glucose has been comparatively investigated at both GCNT/GOx/GAD and DCNT/GOx/GAD film modified GCEs in oxygenated PBS. Fig. 6(a) shows that in the presence of low glucose concentration (0.05 μM), a higher catalytic reduction current corresponding to oxygen reduction is noticed at GCNT/GOx/GAD composite film than that of DCNT/GOx/GAD film on GCE (Fig. 6(a′)). This result shows that the composite film possesses higher electrocatalytic activity for glucose. Similarly, in the presence of high glucose concentration (4.3 μM) the catalytic reduction current observed at the composite film significantly decreases (see Fig. 6(b)). Thus glucose has been effectively oxidized at the composite film. This electrocatalytic response towards glucose is higher than that observed at DCNT/GOx/GAD film or bare/GCE (see Fig. 6(b′) and (c)). This shows the efficient electrocatalytic ability of the composite film towards glucose oxidation. Fig. 6 inset shows the linear dependence of peak currents on various glucose concentration additions at GCNT/GOx/GAD and DCNT/GOx/GAD film modified GCEs. From the inset plot the correlation coefficients of GCNT/GOx/GAD and DCNT/GOx/GAD film modified GCEs are obtained as 0.9946 and 0.9666. Similarly, their sensitivity values are 3.60 and 0.80 μA mM^{-1} cm^{-2}, respectively. The higher sensitivity obtained at the composite film shows the good catalytic efficiency of GCNT than DCNTs. The proposed GCNT/GOx/GAD composite film modified GCE exhibits good electrocatalytic response in the linear concentration range from 1.04 to 3.76 mM of glucose.

3.7. Amperometric determination of glucose at GCNT/GOx/GAD composite film modified GCE

Fig. 7 shows the amperometric i–t curve recorded at GCNT/GOx/GAD composite film modified rotating disc GCE in oxygenated PBS. The electrode potential is kept constant at −0.44 V. Small shoulder peaks appeared immediately for the successive addition of minimum glucose concentrations (0.01 and 0.02 mM), as indicated by arrows in Fig. 7 lower inset. These shoulder peaks appeared as a result of oxygen reduction. With further increase in glucose addition, the oxygen consumption increases and thus the catalytic current decreases gradually and finally levels off for very high glucose concentration (25.84 mM) (see Fig. 7 upper inset). The fabricated GCNT/GOx/GAD composite film modified GCE exhibits steady amperometric response towards glucose in the linear concentration range of 6.30 to 20.09 mM. The correlation coefficient is 0.9995. The sensitivity value at the composite film is 2.47 μA mM^{-1} cm^{-2} for glucose. In Table 1, the electroanalytical values observed at the GCNT/GOx/GAD composite film in this work are comparatively presented with other GOx modified electrodes reported previously [19,26–30]. From Table 1 it is clear that GCNT/GOx/GAD composite film possesses good linear range (6.30–20.09 mM) for glucose which is significantly higher than the linear range obtained at other GOx modified electrodes (see Table 1). The other GOx modified electrodes used for comparison are GOx immobilized at carbon nanotube-gold colloid composites with PDDA coatings

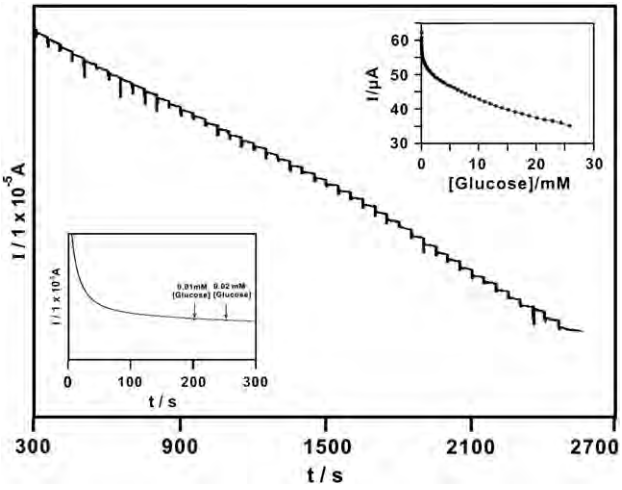

Fig. 7. Amperometric i–t response at GCNT/GOx/GAD composite film modified rotating disc GCE for the addition of 0.01 to 25.84 mM glucose into continuously stirred oxygenated PBS. Applied potential: −0.44 V; rotation rate: 900 RPM. The upper inset shows the plot of linear dependence of peak current with [glucose]/mM. The lower inset shows the enlarged view of amperometric i–t response noticed at GCNT/GOx/GAD composite film within 300 s for 0.01 and 0.02 mM glucose concentration additions into continuously stirred oxygenated PBS.

(GCE/CNT/Au/PDDA-GOx), gold nanoparticles-MWCNT multi layer membrane (GNP/MWCNTs/GOx), poly pyrrole functionalized MWCNTs (PPy-cMWCNTs-GOx), multilayer membrane with sodium dodecyl sulfate functionalized MWCNT and PDDA on 3-mercapto-1-propane-sulfonic acid, sodium salt self assembled gold/titanium deposited poly (ethylene terephthalate) substrate $[GOx/PDDA]_3$/$[SDS\text{-}MWCNT/PDDA]_3$-/MPS/Au/Ti/PET, poly(toluidine blue O) on CNT film (GCE/CNT/PTBO-GOx) and chitosan-$NdPO_4$ nanoparticles composite film (GOx/$NdPO_4$ NPs/CHIT). The good linear range and the excellent electrocatalytic ability of the GCNT/GOx/GAD composite film reported in the present study could be attributed to the good biocompatibility of GCNT matrix for GOx.

3.8. Stability and interference studies

Fig. S4 shows the stability plot of GCNT/GOx/GAD composite film modified GCE stored in PBS at 4 °C for 4 consecutive weeks. About 96.37% peak current is retained at the composite film even after 2 weeks storage in PBS. However, the peak current drops significantly in the consecutive weeks. This result reveals that the composite film exhibits a reasonable stability for two weeks. Here, the good stability of GCNT/GOx/GAD composite film could be attributed to the stability of GCNT.

The selectivity of the developed sensor is mandatory especially for the determination of glucose from serum samples. In human serum, glucose is present with other common interferences like ascorbic acid (AA), uric acid (UA), acetaminophen (AP), pyruvate (PA) and lactate (LA). The normal physiological levels of glucose, AA and AP in human serum are about 5, 0.2 and 0.1 mM respectively [31,32]. Similarly the normal level of lactate in the human serum is 0.52 ± 0.33 mM [33]. Since the normal level of most of the common interferences in human serum is within 0.5 mM, we have used the same concentration for the interference study. Similarly, the normal glucose level in human serum (5 mM) has been used. The technique used for the interference study is amperometric i–t curve. It is clear from Fig. S6 that the GCNT/GOx/GAD composite film exhibits a sharp, rapid response towards 5 mM glucose injected into oxygenated PBS. However, no response is observed at the composite film when 0.5 mM of AA, UA, AP, PA and LA is successively injected into the same oxygenated PBS (see Fig. S6). This result shows that the GCNT/GOx/GAD composite film is highly selective towards glucose determination. This validates that the composite film is suitable for the selective glucose determination in human serum under physiological conditions.

Table 1
Comparison of electroanalytical values for glucose oxidation at various GOx modified electrodes.

Film type	E_{pa} (V) i–t	Sensitivity	Correlation coefficient	Linear concentration range in mM	Ref.
GCE/CNT/Au/PDDA-GOx	−0.3	3.96 mA M^{-1} cm^{-2}	–	0.5–5	[19]
GNP/MWCNTs/GOx	−0.2	7.3 mA mM^{-1} cm^{-2}	0.994	up to 9	[26]
PPy-cMWCNTs-GOx	+0.9	95 nA mM^{-1}	–	up to 4	[27]
$[GOx/PDDA]_3$/$[SDS\text{-}MWCNT/PDDA]_3$−/MPS/Au/Ti/PET	+0.6	5.6 µA mM^{-1} cm^{-2}	0.998	0.02–2.2	[28]
GCE/CNT/PTBO-GOx	−0.1	14.5 mA mM^{-1} cm^{-2}	–	1–7	[29]
GOx/$NdPO_4$ NPs/CHIT	+0.4	1.92 µA mM^{-1}	0.999	0.15–10	[30]
GCNT/GOx/GAD	−0.44	2.47 µA mM^{-1} cm^{-2}	0.9995	6.30–20.09	This work

3.9. Real sample analysis

The practical applicability of GCNT/GOx/GAD composite film has been corroborated through real sample analysis. The technique used is amperometric i–t curve. Serum samples were collected from a healthy woman. During amperometric experiments, definite volume of serum was injected into continuously stirred oxygenated PBS containing GCNT/GOx/GAD composite film modified rotating GCE. The working electrode potential is kept constant at −0.44 V. Fig. S5 shows the amperometric i–t response obtained at GCNT/GOx/GAD composite film modified GCE towards various glucose concentration additions. The composite film exhibits a rapid electrocatalytic response to glucose in the linear range from 0.04 to 0.16 mM (see Fig. S5 inset supplementary data). The correlation coefficient is 0.9781. Further, from the amount of added, found glucose concentrations, recovery has been calculated and the results are given in Table S2. From Table S2 it is clear that the GCNT/GOx/GAD composite film exhibits an excellent average recovery of 97.27% for glucose determination in human serum. The determination of glucose in human serum with good linear range and excellent recovery shows the good practical applicability of the composite film. Further, real sample analysis substantiates the unique ability of the GCNT matrices in promoting the catalytic efficiency of GOx towards glucose.

4. Conclusions

We successfully investigated the direct electrochemistry of GOx at GCNT modified GCE. More stable aqueous dispersion of MWCNT was prepared by wrapping the hydrophobic walls of MWCNT with gelatin. The prepared GCNT was used as a novel matrix for GOx immobilization. GCNT present in the composite film greatly facilitates the electron transfer processes between GOx and GCE. The developed glucose biosensor possesses significant characteristics like good biocompatibility, excellent selectivity, reasonable stability, rapid response, promising electrocatalytic activity towards glucose with good linear range. Moreover, it exhibits rapid electrocatalytic response towards glucose in human serum samples without any common interference at physiological pH. The excellent recovery achieved at the composite film shows the robust performance of the developed biosensor towards glucose determination.

Acknowledgements

This work was supported by the National Science Council and the Ministry of Education of Taiwan (Republic of China).

Appendix A. Supplementary data

Supplementary data associated with this article can be found, in the online version, at doi: 10.1016/j.bioelechem.2010.06.009.

References

[1] M. Musameh, J. Wang, A. Merkoci, Y. Lin, Low-potential stable NADH detection at carbon nanotube-modified glassy carbon electrodes, Electrochem. Commun. 4 (2002) 743–746.
[2] R.T. Kachoosangi, M.M. Musameh, I.A. Yousef, J.M. Yousef, S.M. Kanan, L. Xiao, S.G. Davies, A. Russell, R.G. Compton, Carbon nanotube-ionic liquid composite sensors and biosensors, Anal. Chem. 81 (2009) 435–442.
[3] B. Wu, G. Zhang, Y. Zhang, S. Shuang, M.M.F. Choi, Measurement of glucose concentrations in human plasma using a glucose biosensor, Anal. Biochem. 340 (2005) 181–183.
[4] V. Serafin, L. Agui, P.Y. Sedeno, J.M. Pingarron, Glucosinolate amperometric bienzyme biosensor based on carbon nanotubes-gold nanoparticles composite electrodes, Electroanalysis 21 (2009) 1527–1532.
[5] B. Wu, S. Hou, M. Yu, X. Qin, S. Li, Q. Chen, Layer-by-layer assemblies of chitosan/multi-wall carbon nanotubes and glucose oxidase for amperometric glucose biosensor applications, Mater. Sci. Eng. C 29 (2009) 346–349.
[6] D. Ragupathy, A.I. Gopalan, K. Lee, Synergistic contributions of multiwall carbon nanotubes and gold nanoparticles in a chitosan-ionic liquid matrix towards improved performance for a glucose sensor, Electrochem. Commun. 11 (2009) 397–401.
[7] S. Wang, L. Lu, M. Yang, Y. Lei, G. Shen, R. Yu, A novel cobalt hexacyanoferrate nanocomposite on CNT scaffold by seed medium and application for biosensor, Anal. Chim. Acta 651 (2009) 220–226.
[8] R.B. Rakhi, K. Sethupathi, S. Ramaprabhu, A glucose biosensor based on deposition of glucose oxidase onto crystalline gold nanoparticle modified carbon nanotube electrode, J. Phys. Chem. B 113 (2009) 3190–3194.
[9] D. Wen, X. Zou, Y. Liu, L. Shang, S. Dong, Nanocomposite based on depositing platinum nanostructure onto carbon nanotubes through a one-pot, facile synthesis method for amperometric sensing, Talanta 79 (2009) 1233–1237.
[10] S. Deng, G. Jian, J. Lei, Z. Hub, H. Ju, A glucose biosensor based on direct electrochemistry of glucose oxidase immobilized on nitrogen-doped carbon nanotubes, Biosens. Bioelectron. 25 (2009) 373–377.
[11] C. Xiao, X. Chu, B. Wu, H. Pang, X. Zhang, J. Chen, Polymerized ionic liquid-wrapped carbon nanotubes: the promising composites for direct electrochemistry and biosensing of redox protein, Talanta 80 (2010) 1719–1724.
[12] L. Agui, P.Y. Sedeno, J.M. Pingarron, Role of carbon nanotubes in electroanalytical chemistry, Anal. Chim. Acta 622 (2008) 11–47.
[13] L. Yurong, L.M. Geever, J.E. Kennedy, C.L. Higginbotham, P.A. Cahill, G.B. McGuinness, Thermal behavior and mechanical properties of physically cross-linked PVA/gelatin hydrogels, J. Mech. Behav. Biomed. Mater. 3 (2010) 203–209.
[14] W. Zheng, Y.F. Zheng, Gelatin-functionalized carbon nanotubes for the bioelectrochemistry of hemoglobin, Electrochem. Commun. 9 (2007) 1619–1623.
[15] L. He, Q.W. Di, L.C. Hua, L.L. Bai, Z.G. Li, A novel gelatin-carbon nanotubes hybrid hydrogel, Macromol. Biosci. 3 (2003) 720–724.
[16] S. Haider, S. Park, K. Saeed, B.L. Farmer, Swelling and electroresponsive characteristics of gelatin immobilized onto multi-walled carbon nanotubes, Sens. Actuators B 124 (2007) 517–528.
[17] C. Shan, H. Yang, J. Song, D. Han, A. Ivaska, L. Niu, Direct electrochemistry of glucose oxidase and biosensing for glucose based on graphene, Anal. Chem. 81 (2009) 2378–2382.
[18] A. Salimi, E. Sharifi, A. Noorbakhsh, S. Soltanian, Immobilization of glucose oxidase on electrodeposited nickel oxide nanoparticles: direct electron transfer and electrocatalytic activity, Biosens. Bioelectron. 22 (2007) 3146–3153.
[19] Y. Yao, K. Shiu, Direct electrochemistry of glucose oxidase at carbon nanotube-gold colloid modified electrode with poly(diallyldimethylammonium chloride) coating, Electroanalysis 20 (2008) 1542–1548.
[20] E. Laviron, General expression of the linear potential sweep voltammogram in the case of diffusionless electrochemical systems, J. Electroanal. Chem. 101 (1979) 19–28.
[21] N. Jia, L. Liu, Q. Zhou, L. Wang, M. Yan, Z. Jiang, Bioelectrochemistry and enzymatic activity of glucose oxidase immobilized onto the bamboo-shaped CNx nanotubes, Electrochim. Acta 51 (2005) 611–618.
[22] D. Wen, Y. Liu, G. Yang, S. Dong, Electrochemistry of glucose oxidase immobilized on the carbon nanotube wrapped by polyelectrolyte, Electrochim. Acta 52 (2007) 5312–5317.
[23] S. Zong, Y. Cao, H. Jua, Direct electron transfer of hemoglobin immobilized in multiwalled carbon nanotubes enhanced grafted collagen matrix for electrocatalytic detection of hydrogen peroxide, Electroanalysis 19 (2007) 841–846.
[24] J. Wang, Electrochemical glucose biosensors, Chem. Rev. 108 (2008) 814–825.
[25] R. Garjonyte, A. Malinauskas, Amperometric glucose biosensor based on glucose oxidase immobilized in poly (o-phenylenediamine) layer, Sens. Actuators B 56 (1999) 85–92.
[26] Y. Liu, S. Wu, H. Ju, L. Xu, Amperometric glucose biosensing of gold nanoparticles and carbon nanotube multilayer membranes, Electroanalysis 19 (2007) 986–992.
[27] Y. Tsai, S. Li, S. Liao, Electrodeposition of polypyrrole-multiwalled carbon nanotube-glucose oxidase nanobiocomposite film for the detection of glucose, Biosens. Bioelectron. 22 (2006) 495–500.
[28] X.B. Yan, X.J. Chen, B.K. Tay, K.A. Khor, Transparent and flexible glucose biosensor via layer-by layer assembly of multi-wall carbon nanotubes and glucose oxidase, Electrochem. Commun. 9 (2007) 1269–1275.
[29] Y. Yao, K. Shiu, Low potential detection of glucose at carbon nanotube modified glassy carbon electrode with electropolymerized poly (toluidine blue O) film, Electrochim. Acta 53 (2007) 278–284.
[30] S. Qinglin, L. Kai, L. Lei, Z. Jianbin, Direct electrochemistry of glucose oxidase immobilized on $NdPO_4$ nanoparticles/chitosan composite film on glassy carbon electrodes and its biosensing application, Bioelectrochemistry 74 (2009) 246–253.
[31] E. Scavetta, B. Ballarin, D. Tonelli, A cheap amperometric and optical sensor for glucose determination, Electroanalysis 22 (2010) 427–432.
[32] H. Tang, J. Chen, S. Yao, L. Nie, G. Deng, Y. Kuang, Amperometric glucose biosensor based on adsorption of glucose oxidase at platinum nanoparticle-modified carbon nanotube electrode, Anal. Biochem. 331 (2004) 89–97.
[33] T. Nishijima, M. Nishina, K. Fujiwara, Measurement of lactate levels in serum and bile using proton nuclear magnetic resonance in patients with hepatobiliary diseases: its utility in detection of malignancies, Jpn. J. Clin. Oncol. 27 (1997) 13–17.